RESEARCH ARTICLE | JULY 01 2004

Scaling, spectra and zonal jets in beta-plane turbulence

Sergey Danilov; David Gurarie

Physics of Fluids 16, 2592–2603 (2004)
https://doi.org/10.1063/1.1752928

Scaling, spectra and zonal jets in beta-plane turbulence

Sergey Danilov
Alfred Wegener Institute for Polar and Marine Research, 27515 Bremerhaven, Germany and Institute of Atmospheric Physics, 109017 Moscow, Russia

David Gurarie
Case Western Reserve University, Cleveland, Ohio 44106

(Received 19 November 2003; accepted 25 March 2004; published online 4 June 2004)

A beta-plane approximation of the two-dimensional quasigeostrophic model describes a single layer (barotropic) fluid subjected to a latitudinally varying Coriolis parameter or topography. Rhines (1975) initiated the study of beta-plane turbulence. He predicted the inverse energy cascade into predominantly zonal modes, hence an array of eastward–westward jets, and estimated the jet number (celebrated Rhines scale). He also proposed a k^{-5} scaling law of zonal energy spectra. Our paper re-examines scaling, spectra, and zonal structure of beta-plane turbulence, based on theoretical predictions and numeric experiments. We show that the inverse cascade gives rise to strong organized zonal jets that evolve a peculiar frontal-band (''saw-tooth'') vorticity profile. Such structure affects all spectral properties of the system, by creating organized sequences of spectral peaks, and thus confounds any putative ''scaling behavior.'' The frontal-band structure appears consistently in all stochastically forced beta-plane flows, independent of dissipation and/or other details. But the resulting turbulent quasiequilibrium is not unique, its gross parameters (jets number, mean vorticity gradient) retain memory of the initial state and/or history. © *2004 American Institute of Physics.* [DOI: 10.1063/1.1752928]

I. INTRODUCTION

Large-scale geophysical flows are approximately two-dimensional (2D), and can be described by a quasigeostrophic vorticity equation with a beta term[1]

$$\partial_t \zeta + J(\psi,\zeta) + \beta \partial_x \psi = D\zeta + F. \tag{1}$$

Here ψ denotes stream function, $\zeta=\Delta\psi$, relative vorticity; $J(\psi,\zeta)=\psi_x\zeta_y-\psi_y\zeta_x$, standard Jacobian; D, dissipation operator (a combination of frictional and viscous terms); and F, forcing. The beta term comes from the latitudinal variation of the Coriolis parameter $f=f_0+\beta_y$ (y, northward direction), while source F arises in many applications, from the underlying instabilities (baroclinic or convective), and is confined to small scales.

The beta-plane system (1) and similar one on the rotating sphere were proposed as a plausible explanation of persistent zonal jets on giant planets and in the world ocean.[2–9]

In general, unforced nondissipative fluids described by (1) conserve energy and enstrophy. So one expects two energy fluxes (up and down the forcing scale): the direct *enstrophy cascade*, and the inverse *energy cascade*.[10] The inverse cascade in a typical 2D system will drive the energy up to large scales, and dissipate it by friction. A strong beta term (1) however, can modify the upward flux by creating strong anisotropy and channelling the bulk of energy into preferentially zonal modes.[11–16] The net result are strong zonal jets, observed in nature (giant planets, oceans), and in numeric simulations of beta-plane turbulence.

Rhines' paper[11] initiated the study of beta-plane turbulence, and introduced his celebrated scale,

$$k_{\mathrm{Rh}} = \sqrt{\frac{\beta}{2V_{\mathrm{rms}}}}, \tag{2}$$

expressed through rms velocity V_{rms} and the beta coefficient. Scale k_{Rh} was suggested as the halting scale of the inverse cascade. Rhines based his argument on balance between nonlinear and beta terms (1), and looked for an explanation of zonal tendency in terms of ''Rossby wave radiation.'' This led him to the following relation between wave numbers $k \sim k_{\mathrm{Rh}}$, the energy content of the kth shell and β:

$$E(k) = C\beta^2 k^{-5}. \tag{3}$$

Strictly speaking (3) should be viewed as an estimate for k_{Rh}. However, Rhines proposed a putative ''equilibrium spectrum'' of beta-plane turbulence given by (3).[17]

Subsequent studies have corroborated and clarified Rhines' theory. The basic mechanism of zonal tendency and inhibition of nonzonal modes was linked to ''frequency detuning'' of triad interactions, rather then ''Rossby wave radiation'' (see Refs. 8, 12, and 14).

While many studies validated (2) as an estimate of ''jet-number'' and ''energy peak'' scale, the scaling relation (3) proved much harder to establish analytically or numerically. A few recent studies claim to produce such k^{-5} scaling for zonal energy spectra in numeric simulations,[8,9,15,16,18,19] or find it in zonal spectra of giant planets.[9,19]

Despite several claims, no consensus has been found so far on an appropriate regime for the ''k^{-5} law.'' Some[8,15,18] propose frictionless nonstationary turbulence, while others[9,16,20] examine quasistationary regimes, stabilized by bottom friction. Different forcing was employed to stir tur-

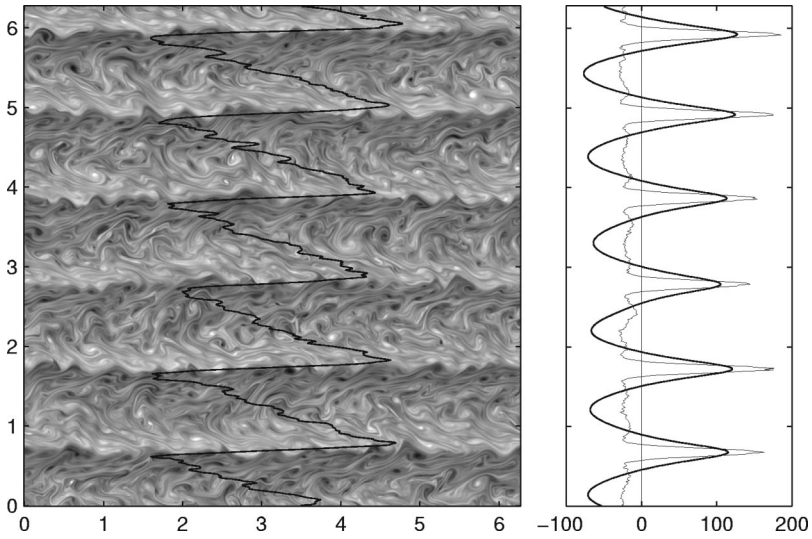

FIG. 1. Left panel, snapshot of the vorticity field in hypofriction run 7 with superimposed instantaneous zonal mean vorticity profile. Abscissa and ordinate are x and y coordinates. The gray palette is from -15 (black) to 15 (white). The vorticity profile is centered around $x=\pi$ and corresponds to $\langle\zeta(y)\rangle/5$. Right panel, $\langle d\zeta(y)/dy\rangle$ (thin line) averaged over 100 units centered around the snapshot time and zonal velocity (thick line) multiplied with 100 to fit the same axes.

bulence, while most authors use short correlated stochastic forcing, Marcus *et al.*[16] apply a steady ''four-mode'' source $F_0\cos(k_f x/\sqrt{2})\cos(k_f y/\sqrt{2})$.

Strictly speaking, the ''universality'' of the k^{-5} scaling implies constant value $C=C_z$ in (3) independent of forcing, dissipation, etc. Yet the above works produced widely divergent estimates of C_z. Specifically, Refs. 8, 15, and 9 estimate it in the range 0.3–0.5, which is an order of magnitude higher than $C_z\approx 0.08$ of Ref. 16.

Our paper attempts to re-examine some conventional ideas and results of the beta-plane turbulence,[21,22] focusing on its zonal structure and the effects of frictional dissipation. We show the resulting turbulent quasiequilibrium to depend on a subtle interplay between the beta and friction terms. The former gives rise to Rhines scale (2), the latter defines a frictional scale k_{fr} (5), the ''would-be arrest scale'' in the absence of beta. In Ref. 23 we proposed ratio $\gamma=k_{\mathrm{Rh}}/k_{\mathrm{fr}}$, as a measure of anisotropy, or ''zonal strength'' of the flow (see Sec. II). Indeed, small $\gamma\ll 1$ gives nearly isotropic turbulence, while $\gamma\gg 1$ implies strong zonal regime.

Earlier work[24] studied in detail zonal jets of beta-plane turbulence, and found a peculiar frontal-band (saw-tooth) pattern of the vorticity profile (illustrated in Fig. 1). The sloping sides of the teeth (zones) have nearly constant negative mean gradient $\overline{\partial\zeta/\partial y}=-\beta_*>-\beta$, separated by narrow ''frontal bands'' with steep positive slope. The corresponding zonal mean velocity acquires a piecewise parabolic shape with strong (eastward) jets centered at frontal bands, interlaced with broad shallow westward jets. Similar patterns are routinely found in numeric simulations (see, e.g., Refs. 6 and 15), and observed zonal jets on giant planets (see, e.g., Refs. 3 and 7).

Our paper continues the study of Ref. 24, and examines in detail zonal jet structure on beta plane: its, stability, interaction with turbulent background, the effect of forcing, dissipation, initialization, and its contribution to the energy spectra. We observe frontal bands to appear consistently in all stochastically forced cases,[25] and describe them by two basic parameters: the principal jet number $k_j\approx k_{\mathrm{Rh}}$, and the mean negative slope of zonal vorticity β_*. Frontal bands create regular (quasiregular) sequences of spectral peaks clustered at harmonics of the principal jet number. Those are superimposed on a lower level background spectrum. The entire spectrum (peaks plus background) can vary slowly in time, but these variations do not allow a meaningful ''time averaging'' to produce a ''scaling law.''

Indeed, scaling behavior, if any, should be studied separately for the continuous (background) spectrum, and for peaks' envelope of large scale zonal flow. The peaks' envelope Ref. 24 can be shown to fall off steeper than k^{-4}. Yet the envelope curves and ''universal constants'' C_z prove highly sensitive to forcing and dissipation parameters, a far cry of ''universality.''

The only ''universal feature'' of the beta-plane turbulence found in our experiments is the saw-tooth (frontal-band) pattern of zonal mean vorticity. So any meaningful parametrization of the large scale spectra should account for zonal structure, through its parameters k_j, β_* and a suitable ''shape functions,'' discussed in Sec. V C.

Our paper starts with an overview of the basic beta-plane phenomenology and scaling (Sec. II). Then we outline numeric experiments (Sec. III), examine the frontal band structure of various flow regimes (Sec. V), study its implications for zonal and isotropic spectra (Sec. V C), and conclude with some open problems.

II. BASIC PHENOMENOLOGY

Beta-plane turbulence is modeled by 2D vorticity equation (1) with forcing term F, and dissipation D. The forcing term is usually localized in the vicinity of large wave number k_f, and the dissipation operator combines frictional and viscous terms. For computational purposes, one often applies so-called *hypofriction* and *hyperviscosity*,

$$D=-\lambda_n(-\nabla^2)^{-n}-\nu\nabla^{2m}. \tag{4}$$

The former (λ-term) serves to suppress the upscale energy cascade, the latter (viscosity) halts the downscale enstrophy cascade.

TABLE I. Parameters of runs.

Run	λ_n	β	$\epsilon 10^4$	E	E_z/E	k_j	k_{Rh}	t_i	C_z	β_*	t_e	γ
10	0.1	640	24	0.012	0.2	34	45	760	0.015	0.08	5	1.4
20	0.01	640	24	0.12	0.55	19	25	670	0.07	0.18	50	25
30	0.03	80	24	0.04	0.2	10	12	300	0.018	0.1	16	2.2
40	0.005	80	24	0.24	0.46	6	7.6	3300	0.07	0.14	100	21
52	123	320	24	0.49	0.93	16	12.6	1500	0.61	0.5	265	
62	123	80	24	0.135	0.75	11	8.8	850	0.22	0.4	60	
72	25.6	40	30	0.24	0.76	6	5.4	1225	0.3	.38	25	
8	0	320	24	0.97	0.65	10	10.6	900	0.27	<0.7		
92	123	320	24	0.46	0.93	16	12.5	300	0.54	0.5	265	
100	0.01	160	48	0.24	0.42	8	10.7	300	0.04	0.12	50	15
110	0.01	160	48	0.24	0.42	9	10.7	300	0.04	0.14	50	15
120	0.01	320	48	0.24	0.55	11	15.2	1300	0.05	0.13	50	21
130	0.01	160	64	0.32	0.85	7	10	2300	0.12		50	16

The natural physical dissipation in 2D (or quasi-2D) flows is due to bottom (Ekman) friction, which correspond to $n=0$. Such friction damps equally all modes, with large and small scales. Hypofriction $n>0$ (negative power of Laplacian) was proposed in Refs. 8, 15, and 26 for theoretical purposes (turbulent phenomenology). It suppresses selectively the gravest modes of the system and recreates a dissipation-free (inertial) interval in the energy range, but it has no direct physical relevance.

A. Rhines scale and zonal regimes

The Rhines phenomenology explores the balance between nonlinear and beta terms of (1), but leaves out large-scale dissipation. Here we stress the importance of both stabilizing factors: beta and friction (see Ref. 23). Indeed, the beta term alone cannot halt the inverse cascade, but serves only to redirect it to zonal and near-zonal modes, while friction can do it with or without beta.

The friction scale for the bottom-drag case can be computed in terms of the saturation energy of the flow: $E_s=\epsilon/(2\lambda_0)=\epsilon t_e$, a consequence of the energy balance. Indeed, neglecting viscous dissipation we have $\partial_t E=-2\lambda_0 E+\epsilon$, where ϵ is energy production rate; λ_0, friction coefficient; and $t_e=(2\lambda_0)^{-1}$, energy e-folding time. Assuming the standard inverse cascade spectrum, $E(k)=C_K\epsilon^{2/3}k^{-5/3}$ with the Kolmogorov constant $C_K\approx 6$ (between forcing scale k_f and the energy peak k_{fr}), we can estimate the latter as

$$k_{\mathrm{fr}}=(3C_K)^{3/2}(\lambda_0^3/\epsilon)^{1/2} \tag{5}$$

(see Refs. 16, 20, 22, and 27).

Let us note that Kolmogorov-type $k^{-5/3}$-spectra appear naturally in the f-plane turbulence ($\beta=0$) stabilized by bottom drag, and there k_{fr} can serve as the halting scale of the inverse cascade (see, e.g., Ref. 22). But strong β can push the Rhines scale (2) above k_{fr}. In that case k_{Rh} takes over as the halting scale and determine both the energy peak and the jet number of the flow.

The original Rhines formulation of the "halting scale" (2) has limited prognostic use as it relies on unspecified rms velocity $V_{\mathrm{rms}}=\sqrt{2E_s}$ (or the energy content of the flow) and exploits only one external parameter β. The friction term allows one to estimate the total energy E_s, hence V_{rms}, in terms of the external parameters: energy production and dissipation. Thus we get the modified form of the Rhines scale,[23,20]

$$k_{\mathrm{Rh}}=\beta^{1/2}(\lambda_0/4\epsilon)^{1/4}. \tag{6}$$

Depending on the ratio of the two scales (5) and modified Rhines (6), two scenarios are possible.[20,23] For $k_{\mathrm{fr}}\gg k_{\mathrm{Rh}}$ friction would halt the cascade before it could reach the Rhines' scale, which results in nearly isotropic $k^{-5/3}$ turbulence in the range $[k_{fr};k_f]$. On the opposite extreme $k_{\mathrm{fr}}\ll k_{\mathrm{Rh}}$, the strong beta-term distorts the isotropy (and $k^{-5/3}$ scaling), the energy spectra develops a bulge near k_{Rh}, and k_{Rh} takes over as the "halting scale" of the inverse cascade. The ratio of two scales

$$\gamma=k_{\mathrm{Rh}}/k_{\mathrm{fr}}=(3C_K)^{-3/2}2^{-1/2}(\beta^2\epsilon/\lambda^5)^{1/4} \tag{7}$$

can serve as a measure of zonal anisotropy.[23] Accordingly, we define strong ($\gamma\gg 1$) and weak ($\gamma\ll 1$) zonal regimes of beta-plane turbulence. Let us note that parameter γ correlates with other indicators of zonal strength, like zonal share of the total energy (see Table I). It shows higher sensitivity to the friction coefficient, $\gamma=O(\lambda^{5/4})$, rather than to the energy production rate ϵ.

Parameter γ is further elucidated by estimating the anisotropic fraction E_a of total energy E_s,

$$E_a/E_s\approx 1-\gamma^{-2/3}. \tag{8}$$

Indeed, if β were zero, E_a would fill in the range between k_{fr} and k_{Rh} of the standard $-5/3$ turbulent spectrum. So E_a/E_s approaches 1, at large γ. As zonal energy E_z makes up a fraction of E_a, (8) also sets an upper bound on E_z/E_s, and our numerical results (Table I) corroborate these findings.

B. Rhines scale for various friction models

Here we shall briefly discuss a few other versions of the forced-dissipative beta-plane systems and related scales.

1. Hypofriction

The hypofriction case $\lambda_n\nabla^{-2n}$ can be treated similarly to Sec. II A. We still use the energy balance, $\partial_t E=-2\lambda_n\int k^{-2n}E(\mathbf{k})d\mathbf{k}+\epsilon$, integrated over resolved wave numbers. But to get the equilibrium energy E_s we need to

know its spectrum $E(\mathbf{k})$. Let us note that "hypofriction" spectra deviate strongly from the $k^{-5/3}$ law (they are much steeper).[26] To get an approximate solution we estimate the hypofriction by its peak value at the energy spectral peak $k_p \approx k_j$. Thence follows the *e*-folding time, $t_e = (2\lambda_n)^{-1} k_p^{2n}$, and the saturation energy $E_s = \epsilon t_e$ (see Sec. VI). Of course, to compute t_e we need an estimate of the energy peak, for instance $k_p \approx k_{\mathrm{Rh}}$. Substituting $E_s \approx E(k_{\mathrm{Rh}})$ into the Rhines formula (2), we get a hypofriction analog of the modified Rhines scale (6), $k_{\mathrm{Rh}}^{2+n} = \beta \lambda_n^{1/2}/(4\epsilon)^{1/2}$, and the corresponding *e*-folding time $t_e = k_{\mathrm{Rh}}^{2n}/(2\lambda_n)$. Clearly, a large hypofriction order n makes k_{Rh} less sensitive to ϵ, λ. One could also define the hypofriction analog of k_{fr} (for $\beta = 0$), as $k_{\mathrm{fr}} = C(\lambda_n^3/\epsilon)^{1/(2+6n)}$ (with C a constant), and use parameter $\gamma = k_{\mathrm{Rh}}/k_{\mathrm{fr}}$ as a measure of anisotropization (zonal tendency of the flow).

2. Frictionless case

The nonstationary (frictionless) case accumulates energy linearly in time $E = \epsilon t$, so its Rhines scale becomes time dependent,[8] $k_{\mathrm{Rh}}(t) = \beta^{1/2}/(8\epsilon t)^{1/4} \sim t^{-1/4}$. Assuming $\beta = 0$ and $k^{-5/3}$ scaling (as in Ref. 28), the energy peak wave number approximately obeys $(3C_K/2)k_p^{-2/3}\epsilon^{2/3} = \epsilon t$. Hence, the peak scale $k_p = (3C_K/2)^{3/2} t^{-3/2} \epsilon^{-1/2}$ decays with time, and the ratio $\gamma = k_{\mathrm{Rh}}/k_p \sim t^{5/4}$ grows, which means a continuous accumulation of anisotropic energy. Of course, such a cascade would reach the box size in finite time, and keep pumping energy in the gravest zonal modes.

3. Related scales

Besides Rhines' definition (2), two other scales were proposed for beta-plane turbulence. Holloway and Hendershott[12] define $k_{\mathrm{HH}} = \beta/\zeta_{\mathrm{rms}}$, in terms of the rms vorticity (rather than velocity), while Vallis and Maltrud[14] set $k_\beta = (\beta^3/\epsilon)^{1/5}$, based on the energy flux. The relation between all three scales is discussed in Ref. 14. Here we shall briefly review them in terms of zonal regimes.

All three scales exploit the balance between the Rossby wave frequency $|\omega_k| = \beta |k_x|/k^2$, and "eddy frequency" estimated via the strain rate: $\sigma_k = (\int_0^k l^2 E(l)\,dl)^{1/2}$, but they differ in the way σ_k is computed. Scale k_β assumes standard $k^{-5/3}$ energy spectrum hence (implicitly) small β. Inserting the appropriate $V_{\mathrm{rms}} = (3C_K)^{1/2} \epsilon^{1/3} k_{\mathrm{Rh}}^{-1/3}$ in (2) we get $k_{\mathrm{Rh}} = (12C_K)^{-3/10} k_\beta$. Such k_β (up to a constant factor) should be considered a limiting case of k_{Rh} (2) for small β (weak zonal regime).

On the contrary, large β would create energetic jets, and pump the bulk of energy into the lowest zonal modes.[24] Hence, $\sigma_k \approx \zeta_{\mathrm{rms}}$, and we recover the k_{HH} scale. Flows dominated by energetic jets, have $V_{\mathrm{rms}} \approx \zeta_{\mathrm{rms}}/k_{\mathrm{HH}}$, so k_{HH} becomes (up to a factor) the Rhines scale $2k_{\mathrm{Rh}}$.

Thus, these other scales are special cases of the Rhines scale (2), $k_{\mathrm{HH}} \approx 2k_{\mathrm{Rh}}$, for strong zonal regime, and $k_\beta \approx 3.6 k_{\mathrm{Rh}}$, for weak (nearly isotropic) regime.

The precise relation of the Rhines scale to the energy peak, or the jet wave number is less obvious. In most experiments (Table I) k_{Rh} comes reasonably close to k_p and k_j. It slightly overestimates the jet wave number for regular bottom friction,[23] while in the hypofriction runs it underestimates k_j.[24] Scale k_β could also mark a threshold, where the isotropic energy spectrum starts to deviate from the standard $-5/3$ law (see Sec. IV).

III. NUMERICAL PROCEDURE AND EXPERIMENTS

We conducted a series of numerical experiments with beta-plane systems, using a dealiased pseudospectral code on a 512^2 $2\pi \times 2\pi$ computational domain with maximal resolved wave number $k_m = 240$. Most runs (1–12 of Table I) use spectrally localized isotropic Markovian sources in a narrow band $[k_f - 2, k_f + 2]$ of principal wave number k_f. Though nonstationary in a strict sense such sources inject inverse cascade energy at a nearly constant rate ϵ.

We took $k_f = 30$ in run 7, and $k_f = 100$ in all other cases. Run 13 differs from the others, it exploits a stationary anisotropic (four-mode) source at $(k_x, k_y) = (\pm 30, \pm 30)$ proposed by Marcus *et al.*,[16] and has a lower resolution of 256^2. We use it to study the effect of temporal correlation on zonal structure and spectra.

The basic input and output parameters are summarized in Table I. They include (1) (hypo) frictional order n and (2) friction coefficient λ_n; (3) coefficient β; (4) energy injection rate ϵ into the range $k < k_f - 2$; (5) total accumulated energy by the end of the run; (6) zonal fraction of the total energy; (7) observed jet wave number k_j; (8) computed Rhines wave number k_{Rh}; (9) duration of run; (10) mean value of constant C_z in a putative k^{-5} "zonal scaling law," averaged over the spectral interval $[k_j, k_f]$ in the energy range; (11) mean negative vorticity gradient of frontal bands over beta, $a = -\beta_*/\beta$ (Sec. V); (12) energy *e*-folding time t_e; (13) ratio of Rhines to friction scales $\gamma = k_{\mathrm{Rh}}/k_{\mathrm{fr}}$ (for bottom-friction runs).

We also varied initialization schemes in our runs. Most runs (1–8) were initialized at zero vorticity, they include four linear drag cases (1–4), three hypofriction cases (5–7), and friction less case 8. Runs 9–12 start at a sinusoidal zonal profile, $\zeta(y) = \zeta_0 \sin(k_j y)$, with jet-number $k_j \approx k_{\mathrm{Rh}}$ and $\zeta_0^2 k_j^{-2}/4 \sim E_s$. They were designed to test the onset and stability of the frontal-band structure, and the memory effects. The forcing and dissipation of run 9 coincide with run 5. Runs 10 and 11 have identical λ, β and forcing, but slightly different initial jet numbers k_j. Run 12 was initialized in highly energetic state (by factor 4) above its expected equilibrium value.

Some experiments (4–6) were reported earlier,[24] and brought here for further analysis and discussion. Time units of Table I are associated with the numerical procedure, and all runs excepting run 9, evolve over a sufficiently long period (usually many times the energy *e*-folding time t_e). All runs but 1 and 3, accumulate a large fraction of zonal energy, which means they attain a strong zonal state.

While our selection falls short of covering the entire "parameter space" of forced-dissipative beta systems, it allows us to draw some interesting conclusions.

IV. BACKGROUND AND ZONAL FLOW

A typical turbulent beta plane flow can be decomposed, according to Refs. 8 and 9 into a featureless $-5/3$ background and an array of zonal jets. We found that such partition however, is compounded by strong nonzonal modes close to the energy peak wave number $k_p \approx k_j$. These near zonal (satellite) modes could be quite energetic and interact strongly with both the background and zonal jets. We demonstrate this partition in Fig. 2 (see also Refs. 8, 15, 16, and 18).

A background spectrum in the Fourier space is computed by removing zonal component $E_z(k)$ of the isotropic spectrum $E(k)$.[29] $E_z(k)$ is defined as contribution from zonal modes in $E(k)$. Figure 3 shows the resulting compensated spectra (the Kolmogorov constant): $C_K' = (E(k) - E_z(k))k^{5/3}\epsilon^{-2/3}$, for runs 4, 6, and 8. Away from spectral peak k_p, its value drops form the expected "isotropic" one $C_K = 6$, to somewhere below 4. A similar drop of the Kolmogorov constant was reported in Ref. 8, and observed in our other runs.

We attribute this drop to nonlocality of the inverse cascade, whereby a fraction $(1-q)$ of the energy flux bypasses the background and goes directly from the source to zonal (or near-zonal) components. The remaining fraction $q<1$ is injected into the background, and creates an effectively lower energy flux $q\epsilon$, hence lower C_K'. Based on such scenario we predict a reduced Kolmogorov constant of the background to be $C_K' = C_K q^{2/3}$.

To verify this hypothesis we compute the background energy flux $q\epsilon$ through "nonzonal" dissipation rate ϵ_{nz} for runs 4 and 6. In run 4 we find $\epsilon_{nz} \approx 0.0011$, while 6 has $\epsilon_{nz} \approx 0.0008$, which correspond to fractions, $q = 0.67$ and 0.47, respectively, hence the reduced Kolmogorov values, $C_K' \approx 4.9$ and 3.6.

Of course, any attempt to quantify better the "background constant" stumbles on ambiguity of the "background-jet" partition, contaminated with low-k (near zonal) satellite modes. We find that our modified Kolmogorov constant matches the observed value C_K' for run 6, but overestimates it for run 4. Such uncertainty with Kolmogorov constant appears in many inverse cascade systems (with or without beta), as soon as energy spectra deviate from the ideal $k^{-5/3}$ behavior in the energy peak (halting) range $k \approx k_p$.

The approximate "$k^{-5/3}$ background" spectrum dominates at high k, while at low k it looks much steeper (due to strong zonal modes or nearly zonal satellites). We can roughly estimate a transition range from the "background" to "zonal" spectrum in the following way. The "background" rms vorticity gradient at a spatial scale $2\pi/k$ is given by $\beta_k = (\int_0^k C_K' p^4 \epsilon^{2/3} p^{-5/3} dp)^{1/2}$. Next we estimate values k, where β_k takes over β, and get a transition wave number $k_\beta' = (10/3C_K')^{3/10} k_\beta \approx k_\beta$.

V. ZONAL BANDS AND ENERGY SPECTRA

A. Long term evolution

Zonal structure appears at an early stage of evolution, whether seeded or not, and persists over the entire duration of the run. In all stochastically forced cases it gradually develops a saw-tooth pattern of relative vorticity field, illustrated in Fig. 1. The equilibration of zonal structure is a slow evolution process, lasting for tens (or more) e-folding periods t_e. We illustrate it (Fig. 2) for the zonal mean vorticity profiles and energies (total and zonal) in several cases: (a)–(b) for "bottom friction" run 4 (zero initialization); (c)–(d) run 12 (sinusoidal initialization); (e)–(f) "frictionless" run 8. In case (a)–(b) the zonal structure has not yet fully stabilized by the end of $33t_e$-long run, and we observe several jet mergers before the flow settles down at $k_j = 6 \approx k_{\mathrm{Rh}}$. The "sinusoidal" case (c)–(d) maintains a regular periodic zonal array at the fixed (initial) wave number k_j, but slowly evolves a saw-tooth pattern. The unsteady frictionless case (e)–(f) undergoes a succession of jet mergers, that will eventually bring k_j down to 1. Here the frontal bands are less regular, but qualitatively remain "saw-tooth" over long periods between mergers.

The entire zonal structure evolves in the process resembling shock formation in nonlinear (Burgers-type) equations. We observe it for different initializations, either zero (in most runs) or sinusoidal profiles of runs 9–12, whose initial jet number k_j and zonal energy were chosen close to the expected values k_{Rh} and E_z.

The build up of the saw-tooth structure in the vorticity field is most apparent in sinusoidal cases as illustrated in Fig. 4. It takes less than one e-folding period t_e.

Runs 10 and 11 exhibit yet another feature of the beta-plane turbulence—persistent memory of the initial state. Indeed, both have identical forcing/dissipation, but slightly different initial jet numbers. Both systems maintained the initial k_j throughout the entire evolution process. It shows that the Rhines scale k_{Rh} can approximate the jet number of the flow, but different k_j in the vicinity of k_{Rh} can form separate "attraction basins." Reference 24 found a similar "nonuniqueness" for hypofriction flows. Such "nonuniqueness" (runs 10 and 11), and memory effects to initial condition (runs 9–12), imply nonergodicity of beta-plane turbulence. It could be related to nonergodicity of the dissipation-free (conservative) beta plane systems.[30]

B. Frontal band structure

The frontal band structure of Fig. 1 along with its vorticity field, was taken at a late stage of run 7. This flow has accumulated a relatively large share of zonal energy ($E_z/E \approx 0.76$). It exhibits well organized zonal bands separated by sharp fronts. The frontal width is determined by undulations (excursions) of the narrow "wavy" contours, separating adjacent bands. It approximately matches a typical vorticity patch injected by the source. In Fig. 1 the frontal width is approximately 0.2, close to the forcing wavelength $2\pi/k_f \approx 0.21$. Let us note that the forcing scale in our runs is close to a dissipation scale, so the frontal width may be set by a combination of two factors. The small-scale irregularities in the "saw-tooth" zonal profile, however have negligible long term effect.

The teeth of zonal vorticity profiles vary in regularity and steepness, depending on the flow regime and initializa-

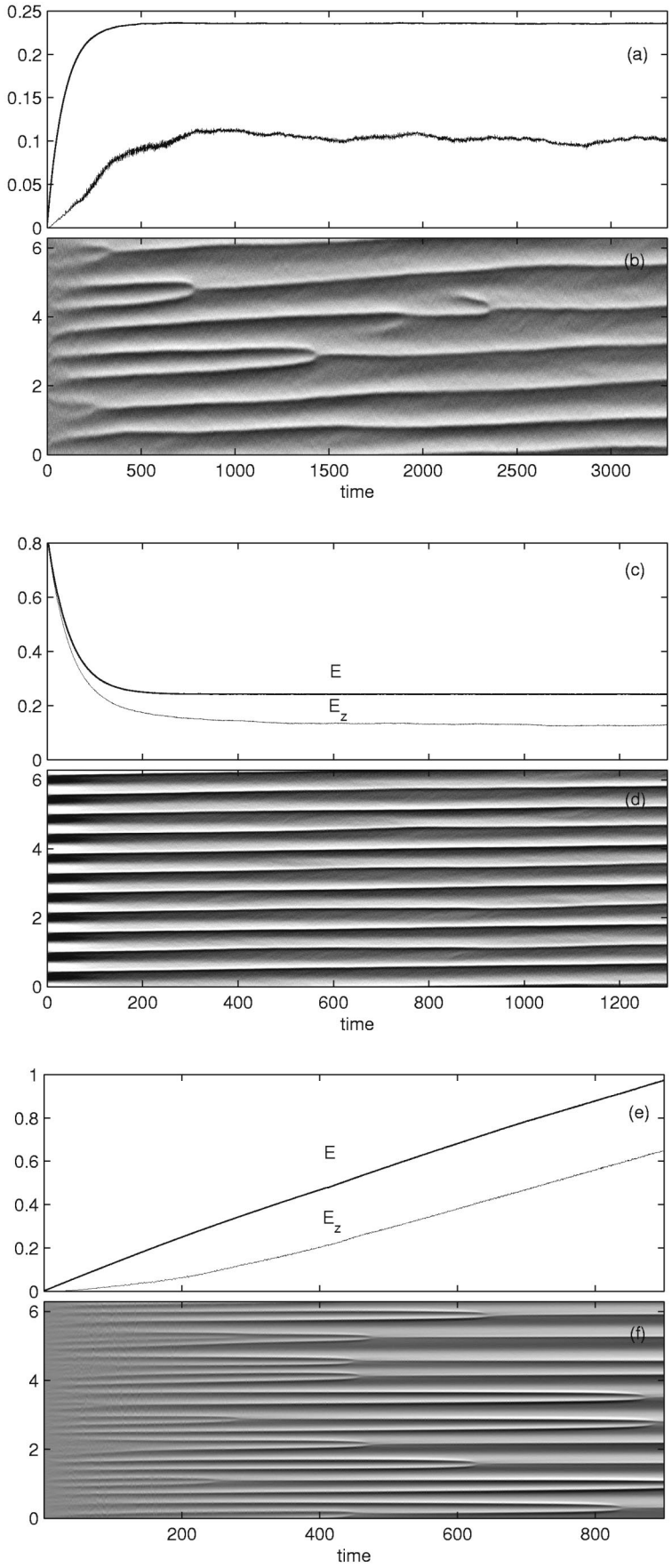

FIG. 2. Long term evolution of energy [(a),(c),(e)] and zonal vorticity [(b),(d),(f)] in bottom-drag runs 4 [(a),(b)], 12 [(c),(d)] and frictionless run 8 [(e),(f)].

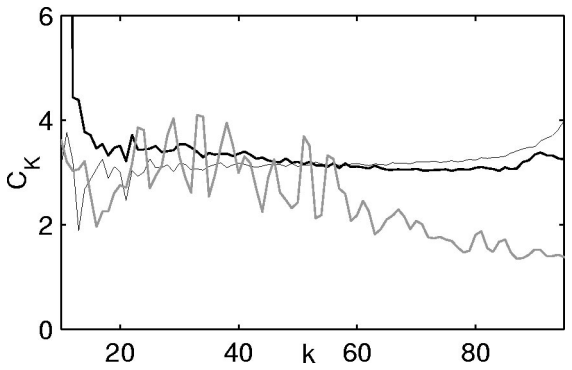

FIG. 3. Kolmogorov constant of the nonzonal component for hypofriction run 6 (thick solid), bottom-drag run 4 (thin solid), and frictionless run 8 (gray). The first two maintain a uniform level $C_K' \approx 3.5$ vs accepted value 6 for the isotropic 5/3 turbulence.

tion. We illustrate it in Fig. 5 for runs 3, 2, 5, 8 (left to right). Weak zonal regime of run 3 [based on its γ-value (7), or the energy fraction E_z/E] exhibits large fluctuations. Increasing zonal strength ($E_z/E \approx 1$) in runs 3 and 5 creates more regular and steep zonal mean vorticity profiles. The frictionless run 8 (right panel) cannot settle, so it combines well-developed vorticity bands with new emerging ones. In all strong zonal cases the frontal width stays close to the forcing scale $2\pi/k_f$ (see also Figs. 1 and 4).

The important parameter of the frontal band structure is the mean (zonally averaged and time averaged) vorticity gradient $\beta_* = -\overline{\partial\zeta/\partial y}$ over a negatively sloping teeth side. According to the Rayleigh–Kuo stability criterion it must be bounded below by $-\beta$. So we can use ratio $a = \beta_*/\beta$ as yet another measure of zonal strength (see Table I). Furthermore, Ref. 24 proposes β_*^2 rather than β^2, as more appropriate for

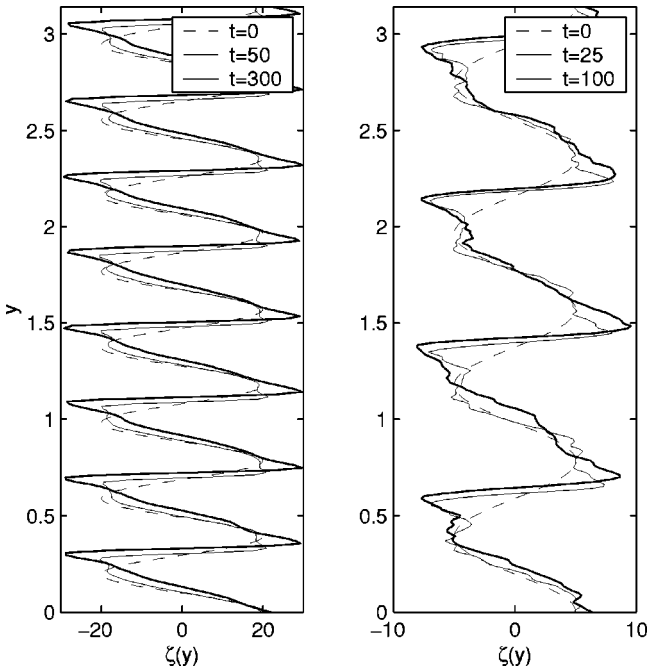

FIG. 4. Evolution of zonal vorticity profiles in runs 9 (left) and 10 (right) initialized with a sinusoidal vorticity distribution. We show one-half of the meridional domain.

zonal spectra, either "scaling laws" like (3) or other properties. Indeed parameter β_* enters explicitly in the idealized saw-tooth pattern discussed below (Sec. V C), hence the total zonal energy of such flow $E_z = (\pi^4/90)\beta_*^2 k_j^{-4}$.

The saw-tooth vorticity profile gives rise to parabolically shaped zonal velocities (over negatively slopping sides of teeth)—westward jets. They meet at frontal regions and create strong narrow eastward jets (see Fig. 1). The zero velocity level in such a flow is set up by the mass conservation. It allows one to estimate the relative strength (peak velocity) and the meridional span of eastward and westward jets[24]

$$\frac{\max(U_{\text{east}})}{\max(U_{\text{west}})} = 2, \quad \frac{\text{Width}(U_{\text{west}})}{\text{Total width}} = \frac{1}{\sqrt{3}}.$$

The ideal "saw-tooth" vorticity profile has infinitely thin (zero width) fronts of infinite positive slope. The fronts observed in our runs have always finite width, which effectively reduces the strength of the eastward jets [see bottom panel (b) of Fig. 5].

A typical hypofriction system stabilizes its frontal-band structure faster $O(t_e)$, than the comparable bottom-drag run, and attains more regular zonal vorticity profile. The difference can be explained by the halting mechanism of two systems. Indeed, the hypofriction arrests the inverse cascade abruptly at $k_j \approx k_p$, hence creates near perfect periodicity. Besides, it suppresses nonzonal satellites below k_j, which speeds up equilibration and yields a higher fraction of zonal energy.

Qualitatively, our profiles of zonal vorticity and velocity agree with other known results on beta plane and rotating sphere under similar conditions (zonal strength E_z/E) of the flow (see Refs. 6 and 15 which present similar patterns of vorticity gradient but do not comment on its structure).

We come to the following general question now: what mechanism could possibly drive slow evolution of zonal vorticity into a saw-tooth pattern? The full details are yet to emerge, but some recent theories of "slow zonal evolution" (Refs. 31 and 32) do not fall within our flow regime, as commented in the Discussion.

We speculate that small scale vorticity patches injected in the beta-plane flow are strained by strong zonal jets, they help to form through their interaction with a virtual "beta shear." This tends to organize vorticity patches in the like of "Karman street," with positive vorticities alinged over the lower (southern) flank of a front, in opposition to negative patch array alone its upper (northern) flank. Two arrays will drive a strong eastward jet within frontal span, and form a perceived "jump discontinuity" of the zonal vorticity profile.

In spectral space, it can be thought of as synchronization (or equilibration) of the principal zonal mode and its harmonics, by the induced four-wave (or possibly higher) interactions, mediated by the background.

C. Zonal spectra: Peaks' envelopes and shape functions

The quasiperiodic frontal band structure of zonal vorticity has immediate implications for the zonal energy spectra. Indeed, Fourier spectrum of any periodic 1D function con-

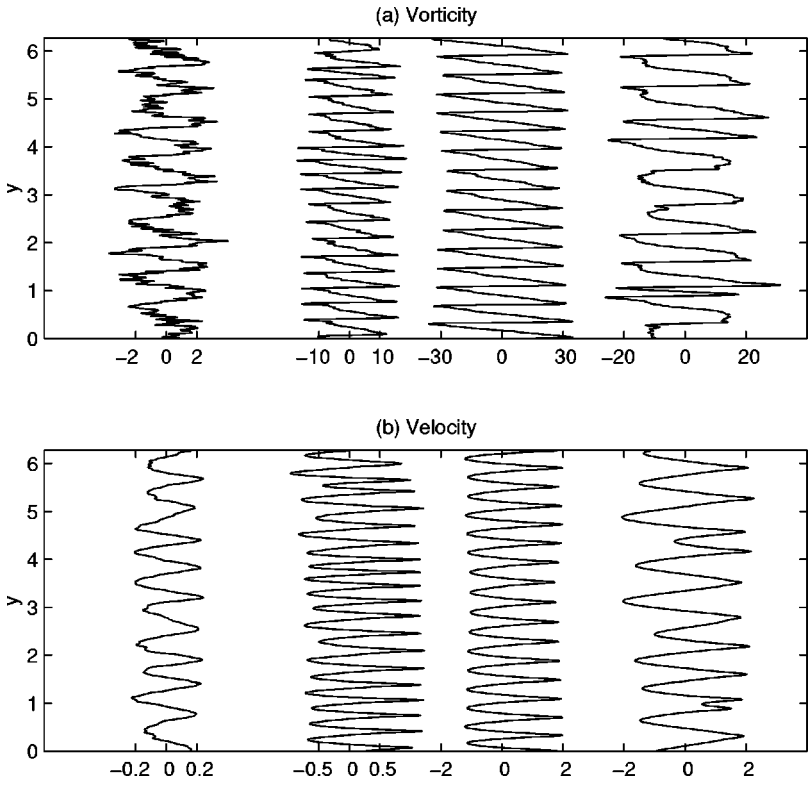

FIG. 5. Instantaneous profiles of the zonal vorticity (a) and zonal velocity (b) fields in bottom-drag runs 3 and 2, hypofriction run 5, and in frictionless run 8 (from left to right).

tains a regular sequence of peaks—harmonics of the principal wave number k_j. Such spectra could be described by a suitable dimensionless shape-function Φ, and two parameters: k_j (jet number) and β_* (mean vorticity gradient $-\overline{\partial_y \zeta}$). The corresponding scaling law will take on the form

$$E_z(k) \sim \frac{\beta_*^2 \Phi(k/k_j)}{k^p k_j^q}, \quad p+q=5 \tag{9}$$

with yet undetermined exponents p and q. Notice that β_*^2 plays here the role of β^2 of (3) (see Refs. 15, 8, and 16).

We shall demonstrate "scaling law" (9) for two idealized examples of the zonal mean vorticity.

(i) *Saw-tooth* of negative slope β_*, with infinitely steep (zero width) fronts,

$$\zeta(y) = -\beta_* \left(y - \frac{2j+1}{N}\pi \right), \quad 0 \leqslant y - \frac{2j+1}{N}\pi \leqslant 2\pi/N \tag{10}$$

for the jth band, $j=1,...,N$. N is the number of vorticity bands, and $k_j = N$ (for 2π domain size).

(ii) *Slopping-tooth profile*,

$$\zeta(y) = \beta_* \begin{cases} -\dfrac{y}{1-\delta}, & \dfrac{\pi}{N}(-1+\delta) < y < \dfrac{\pi}{N}(1-\delta), \\ \dfrac{y-1}{\delta}, & \dfrac{\pi}{N}(1-\delta) < y < \dfrac{\pi}{N}(1+\delta), \end{cases} \tag{11}$$

repeated periodically over the range $0 < y < 2\pi$ with step $2\pi/N$. Here δ is the fraction of the meridional span covered by steep ($\delta \ll 1$) but finite width fronts of positive slope, with the remaining $1-\delta$ fraction covered by bands, like in run 5 (Fig. 5).

Formula (9) gives the exact spectrum of idealized "saw-tooth" jets

$$E_z(k) = \begin{cases} \dfrac{\beta_*^2 \Phi(k/k_j)}{k^4 k_j}, & \text{saw-tooth}, \\ \dfrac{\beta_*^2}{(2\pi\delta(1-\delta))^2} \dfrac{\Phi(k/k_j) k_j}{k^6}, & \text{slopping tooth}, \end{cases} \tag{12}$$

with shape functions

$$\Phi(x) = \begin{cases} N^{-1} \left| \sum_{m=0}^{N} e^{2\pi i m x} \right|^2, & \text{saw-tooth}, \\ N^{-1} \left| \sum_{m=0}^{N} \left(e^{2\pi i (m+\delta-1)x} - e^{2\pi i m x} \right) \right|^2, & \text{slopping tooth}. \end{cases} \tag{13}$$

But there is no way to fix uniquely exponents p, q or shape-function Φ by the standard dimensional arguments, in general.

The saw-tooth profile gives "k^{-4}-scaling"—a consequence of its jump discontinuity. The slopping tooth has continuous ζ, but discontinuous derivative $\zeta'(y)$. Hence the peaks' envelope in (12) scales as k^{-4} for small $k \ll k_j/(2\pi\delta)$ [since $\Phi(x) \sim x^2$ at small x], but changes to k^{-6} at large k. The intermediate range $k_j/(2\pi\delta) < k < k_j/\delta$ has no particular scaling behavior, due to modulation effect ("beats") with period k_j/δ.

The frontal width is approximately equal to the forcing scale, so parameter $\delta \approx k_j/k_f$, and the "k^{-4} scaling" applies to the range $k \ll k_f/(2\pi)$. Combined with the obvious constraint $k > k_j$, only run 4 with $k_j = 6$ could marginally satisfy these conditions. Other cases have poorly defined "slopping range," as $k_j/\delta \approx k_f$.

The above model cases demonstrate a multitude of scaling behavior, and its sensitivity to small scales. The measured profiles in our runs depart from the exact periodicity, and thus do not follow the ideal shape-functions Φ (13). The imperfect periodicity and fluctuations tend to reduce peaks' amplitudes, and fill valleys between the peaks with the continuous background noise. Yet the general "synchronized" peak pattern with an appropriate "shape-function" Φ, persists over long time, and renders untenable any smooth (continuous) "mean spectral curve" with simple scaling.

The measured frontal-band profiles have small-scale irregularities (Fig. 1) superimposed on the mean flow. They have smoothing effect on zonal spectra, but its contribution is limited to large k, far away from the dominant spectral peaks.

VI. ENERGY SPECTRA AND SCALING

Here we shall examine contribution of frontal bands to isotropic and zonal energy spectra, $E(k)$, $E_z(k)$, the zonal component of $E(k)$. Two spectra become nearly identical in the low-k range for strong zonal regimes. The most energetic (low-k) part contains sequences of spectral peaks, due to quasisteady zonal jets, illustrated in Fig. 6 for runs 1, 2, 4, 12, and 6 (top to bottom). The left column contains isotropic and zonal spectra, the right column shows the compensated spectra ("putative constant") $C_z = E_z(k)k^5/\beta$ and their standard deviations. All spectra of Fig. 6 were averaged over many e-folding periods t_e.

Thus the first row of Fig. 6 (run 1) includes the last $100t_e$ units of its entire $150t_e$ span, where it attained a quasistationary equilibrium. Its large friction coefficient λ halts the inverse cascade at a relatively high wave number. A pair of strong peaks, $k = 32$ and $k = 36$, indicates a competition between two principal modes, with 32 being slowly replaced by 36 during the final phase. This case is only marginally zonal, with zonal energy making up 20% of the total energy, and 90% of E_z confined within a narrow range: $30 \leqslant k \leqslant 40$. One can barely discern the second harmonics of the principal peaks. The compensated zonal spectrum (right panel) has relatively small standard deviation at the peaks, but it becomes comparable to spectrum in valley between adjacent peaks, another indication of the persistent long-lived zonal structure. The mean value of "universal constant" $C_z \approx 0.015$, in the range $30 < k < 95$.

Run 2 has smaller friction hence stronger zonal jets, and an increased share of zonal energy, $E_z = 0.55E_t$. The second row of Fig. 6 shows its spectra averaged over the last $8t_e$ units of integration. The system has not yet fully stabilized, while k_j has reached its equilibrium value, vorticity bands keep adjusting. One clearly sees the principal peak and its second harmonic, with relatively low standard deviation (right panel), long-lived organized zonal flow. The principal zonal peak $k_p = 19$ alone carries 24% of the total energy, locked (80%) within range $14 \leqslant k \leqslant 24$. The peaks' envelope resembles the k^{-5} curve on the left panel, but the right panel shows increased oscillation of "constant" C_z, about its mean value ≈ 0.07.

Run 4 [Fig. 2(b)] averaged over the last $15t_e$ units of integration has clearly discernible second and third harmonics of the main peak. The peaks' envelope here is shallower than[33] k^{-5}, and C_z has mean value 0.07 over $6 < k < 30$. As above its standard deviation stays low at the peaks, and the bulk of zonal energy (90%) is locked within range $4 \leqslant k \leqslant 8$.

Run 12 (fourth row of Fig. 6) has a regular array of zonal peaks at the harmonics of $k_j = 11$, with shallow envelope (below k^{-5}) at small $k < 50$, and steeper than k^{-5} at larger k.

We note a common feature of all bottom-drag cases, the presence of strong nonzonal satellite modes with small longitudinal wave numbers, $k_x = 1,2,...$ (near k_y axes). Normally, such satellites have lower "latitudinal" components k_y than the principal zonal peaks, and thus push the isotropic energy peak to smaller k than the principal zonal peak [third row of Fig. 6, and similar pattern in Ref. 18 (Fig. 14)].

The hypofrictional spectra look similar to run 12, but have more regular (periodic) arrays of spectral peaks, and suppressed near zonal satellites. Figure 6 (last row) illustrates it for run 6 averaged over the last $5t_e$ units of integration. Here the peaks' envelope seems to follow the k^{-5} scaling at small k, but falls off steeper at larger k. The principal zonal peak alone contains 93% of the zonal energy. Zonal spectra of runs 4 and 12 (third and fourth rows of Fig. 6) also come close to k^{-5} law over a limited intervals of k with "constant" $C_z \approx 0.04$. Let us also note that the valleys between peaks in run 1 (upper row of Fig. 6) roughly follow such scaling. It disappears however in other cases (second and last rows of Fig. 6). Whatever their "scaling" such continuous (background and zonal) spectra store a negligible amount of energy compared to the mean zonal flow of spectral peaks.

The frictionless turbulence has transient spectra, so Ref. 8 applies ensemble averaging to produce k^{-5} scaling. Such averaging can smooth out unsteady spectra, but it cannot be related to any particular flow realization, or history (no matter how long), as beta-plane turbulence lacks ergodicity (Sec. V A and Ref. 30).

To conclude, our numeric results give no clear indications of "universal scaling" for zonal spectra. But they exhibit a consistent "background plus peaks" pattern best cap-

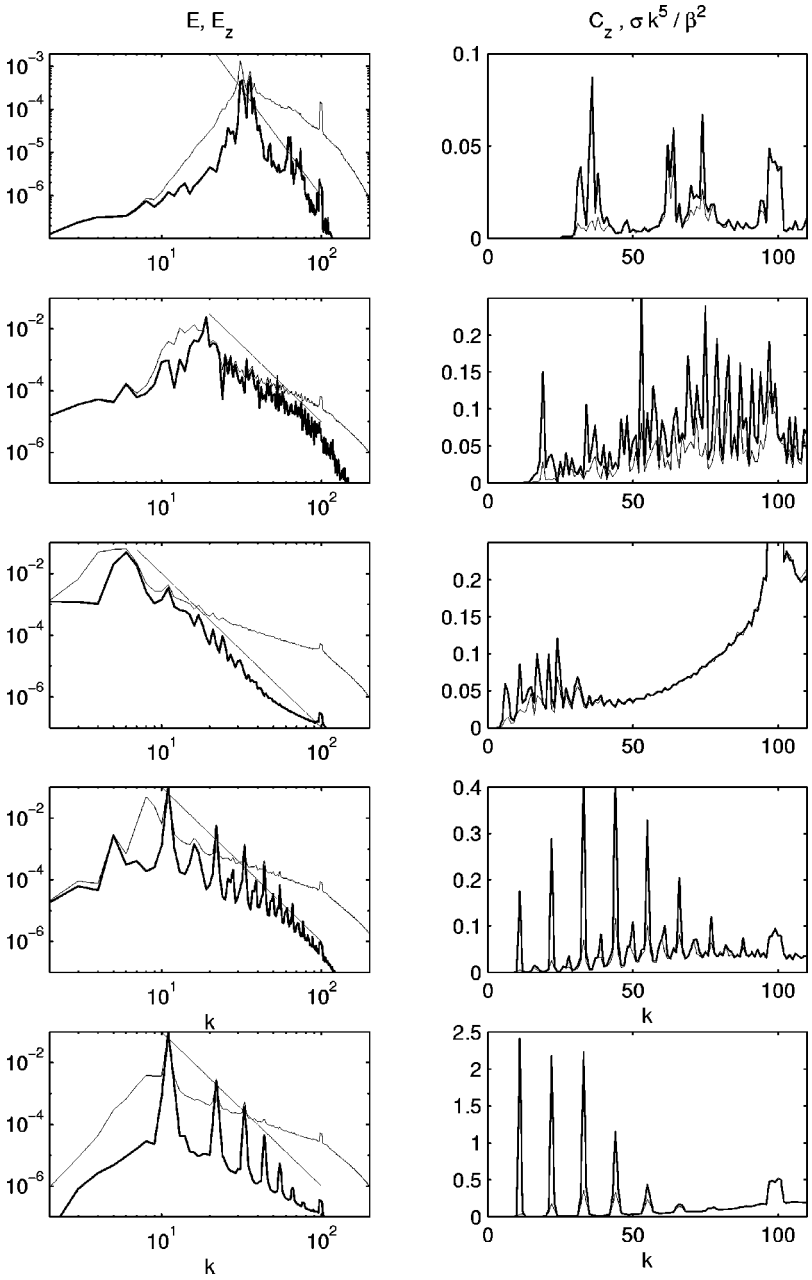

FIG. 6. Isotropic and zonal energy spectra (left) and compensated zonal spectra along with their standard deviations (right) for runs 1, 2, 4, 12, and 6 (from top to bottom). Zonal energy spectra are plotted thick, and straight lines in the left panels correspond to k^{-5} laws. Spectra are averaged over finite time intervals (explained in the text).

tured through suitable shape functions discussed in the preceding section.

VII. DISCUSSION AND CONCLUSIONS

Forced beta-plane turbulence stabilized by large scale friction tends to develop anisotropy and accumulate energy in zonal (or near zonal) modes. One can measure ''zonal anisotropy'' by the ratio of two scales $\gamma = k_{\mathrm{Rh}}/k_{\mathrm{fr}}$ ''Rhines'' (2) over ''frictional'' (5). The latter represents the would-be arrest scale of the inverse cascade in the absence of beta. Weak β and strong friction ($k_{\mathrm{Rh}} \ll k_{\mathrm{fr}}$) give nearly isotropic turbulence ($\gamma \ll 1$) halted at k_{fr}, while strong beta makes k_{Rh} the dominant halting scale.[23]

Strong beta-plane turbulence ($\gamma \gg 1$) develops a periodic/quasiperiodic array of eastward/westward zonal jets at wave number $k_j \approx k_{\mathrm{Rh}}$, and its zonal mean vorticity takes on a saw-tooth (frontal-band) pattern, hence ''parabolic-type'' zonal velocity profile with strong narrow eastward jets, and broad weak westward ones. The negative mean gradient of zonal bands $\beta_* = \overline{\partial\zeta/\partial y}$, is bounded below by $-\beta$.

The frontal band structure appears consistently in all stochastic (or stationary) forced cases (runs 1–12), regardless of the specific friction law (bottom drag, hypo, or zero friction), sources, or initialization. The resulting turbulent quasiequilibrium, however maintains memory of its initial state (initial jet number) and the history of the process.

Zonal jets evolve slowly from the turbulent background, created by the source, through the inverse cascade mechanism. The background has nearly isotropic $-5/3$ spectrum typical of the *f*-plane turbulence, but with lower Kolmogorov constant $C_K' = \epsilon^{-2/3} k^{5/3} (E(k) - E_z(k))$, compared to its ''isotropic value'' $C_K = 6$. We attribute such drop to nonlocality of

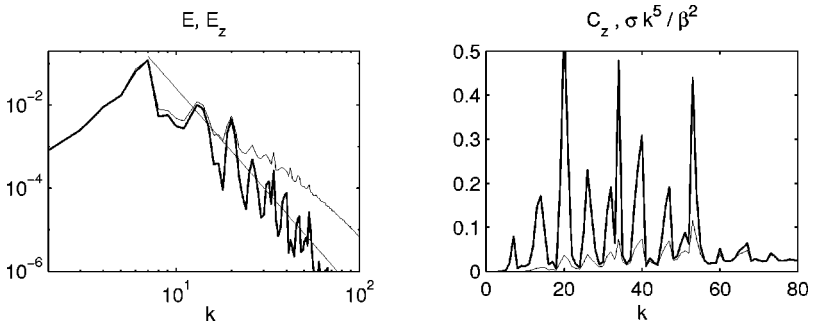

FIG. 7. Same as in Fig. 6 for run 13.

the inverse cascade, whereby a fraction $(1-q)\epsilon$ of the energy output, goes to large scale zonal (or near zonal) modes bypassing the background. The remaining fraction q gives the lower effective energy production injected into the background flow, hence lower Kolmogorov constant $C_K' = q^{2/3} C_K$. We can estimate the "background energy production" $q\epsilon$, by the energy dissipation of nonzonal modes, and it gives a good agreement between the predicted and computed values C_K'.

Stationary arrays of frontal jets give rise to quasiregular sequences of spectral peaks at harmonics of k_j. So typical beta-plane spectrum combines the "5/3 background" and zonal peaks. The latter dominate the low-k energy range, and confound any putative "scaling law." We demonstrate it by two model examples, so-called *saw-tooth* and *slopping-tooth* profiles, described by suitable shape-function Φ. The former yields the k^{-4} scaling for the peaks' envelope, the latter allows a range of exponents between -4 and -6. Besides, the slopes of peaks' envelopes are highly sensitive to minute details of frontal bands and small scales eddies, which renders any "scaling law" untenable.

Our experiments include both stochastic (short correlated) forcing and stationary sources of the type.[16] The latter produce different (from saw-tooth) zonal patterns, but their energy spectra are still dominated by zonal peaks without apparent scaling (cf. Fig. 7).

Frontal bands evolve gradually in a process resembling shock formation in nonlinear "Burgers' type" equations. Their persistence raises a challenging problem of the sustaining mechanism and slow evolution. Two recent works[31,32] develop such "slow evolution" theory for zonal jets of the perturbed Kolmogorov flow in a weakly nonlinear regime. The former[31] does it for plane geometry, the latter[32] considers spherical geometry. Both papers assume negligibly small bottom drag, so viscosity becomes the dominant dissipative factor everywhere except the gravest modes. An instability can set in here at arbitrarily small wave numbers, hence comes small parameter ϵ, and natural "fast" and "slow" variables in the system. Then the multiscale analysis yields a "slow" evolution of Cahn–Hilliard type for the zonal velocity profile $U(y/\epsilon, t/\epsilon^p)$.

Some qualitative predictions of Refs. 31 and 32 agree with our numeric results, but there are fundamental differences in our setup. Zonal jets of Refs. 31 and 32 evolve as weak nonlinear instabilities of "transverse perturbations" subjected to "beta forcing" in "near-frictionless" environment. Such regime is very different form highly nonlinear dissipative-forced turbulence of our experiments. So our zonal jets should evolve as instabilities of the (5/3) turbulent background, rather than weakly unstable transverse jets. There is no yet adequate theory to explain such kind of "instability." While our zonal structure also undergoes slow evolution and equilibration, the nature and origin of "small parameters" and "slow variables" remains unknown, and poses a challenging mathematical problem.

ACKNOWLEDGMENTS

The authors gratefully acknowledge the support of Geophysical turbulence program at NCAR, and stimulating discussions with B. Galperin, V. M. Gryanik, J. Herring, S. Sukoriansky, and G. K. Vallis.

[1] J. Pedlosky, *Geophysical Fluid Dynamics* (Springer-Verlag, Berlin, 1987).
[2] G. P. Williams, "Planetary circulations. 1. Barotropic representation of Jovian and terrestrial turbulence," J. Atmos. Sci. **35**, 1399 (1978).
[3] P. S. Marcus, "Jupiter's Great Red Spot and other vortices," Annu. Rev. Astron. Astrophys. **31**, 523 (1993).
[4] J. Y.-K. Cho and L. M. Polvani, "The emergence of jets and vortices in freely evolving, shallow-water turbulence on sphere," Phys. Fluids **8**, 1531 (1996).
[5] T. Nozawa and S. Yoden, "Formation of zonal band structure in forced two-dimensional turbulence on a rotating sphere," Phys. Fluids **9**, 2081 (1997); "Spectral anisotropy in forced two-dimensional turbulence on a rotating sphere," *ibid.* **9**, 3834 (1997).
[6] H.-P. Huang and W. A. Robinson, "Two-dimensional turbulence and persistent zonal jets in a global barotropic model," J. Atmos. Sci. **55**, 611 (1998).
[7] P. S. Marcus and C. Lee, "A model for eastward and westward jets in laboratory experiments and planetary atmospheres," Phys. Fluids **10**, 1474 (1998).
[8] H.-P. Huang, B. Galperin, and S. Sukoriansky, "Anisotropic spectra in two-dimensional turbulence on the surface of a rotating sphere," Phys. Fluids **13**, 225 (2001).
[9] S. Sukoriansky, B. Galperin, and N. Dikovskaya, "Universal spectrum of two-dimensional turbulence on a rotating sphere and some basic features of atmospheric circulation on giant planets," Phys. Rev. Lett. **89**, 124501 (2002).
[10] R. H. Kraichnan, "Inertial ranges in two-dimensional turbulence," Phys. Fluids **10**, 1417 (1967); "Inertial-range transfers in two- and three-dimensional turbulence," J. Fluid Mech. **47**, 525 (1971).
[11] P. B. Rhines, "Waves and turbulence on a beta-plane," J. Fluid Mech. **69**, 417 (1975).
[12] G. Holloway and M. Hendershott, "Stochastic closure for nonlinear Rossby waves," J. Fluid Mech. **82**, 747 (1977).
[13] M. E. Maltrud and G. K. Vallis, "Energy spectra and coherent structures in forced two-dimensional and beta-plane turbulence," J. Fluid Mech. **228**, 321 (1991).
[14] G. K. Vallis and M. E. Maltrud, "Generation of mean flows and jets on a beta plane and over topography," J. Phys. Oceanogr. **23**, 1346 (1993).
[15] A. Chekhlov, S. A. Orszag, S. Sukoriansky, B. Galperin, and I. Starosel-

sky, ''The effect of small-scale forcing on large-scale structures in two-dimensional flows,'' Physica D **98**, 321 (1996).
[16]P. S. Marcus, T. Kundu, and C. Lee, ''Vortex dynamics and zonal flows,'' Phys. Plasmas **7**, 1630 (2000).
[17]Although he recognized such scaling would violate the locality assumption implicit in derivation of (3).
[18]L. M. Smith and F. Waleffe, ''Transfer of energy to two-dimensional large scales in forced, rotating three-dimensional turbulence,'' Phys. Fluids **11**, 1608 (1999).
[19]B. Galperin, S. Sukoriansky, and H.-P. Huang, ''Universal n^{-5} spectrum of zonal flows on giant planets,'' Phys. Fluids **13**, 1545 (2001).
[20]K. S. Smith, G. Boccaletti, C. C. Henning, I. Marinov, C. Y. Tam, I. M. Held, and G. K. Vallis, ''Turbulent diffusion in the geostrophic inverse cascade,'' J. Fluid Mech. (to be published).
[21]Indeed, ''scaling'' at small k becomes tenuous even for isotropic turbulence (see, e.g., Ref. 22). As for beta plane it requires exceedingly long ''time average'' to produce a semblance of ''power law'' behavior (Refs. 15, 8, and 9).
[22]S. Danilov and D. Gurarie, ''Nonuniversal features of forced two-dimensional turbulence in the energy range,'' Phys. Rev. E **63**, 020203 (2001); ''Forced two-dimensional turbulence in spectral and physical space,'' *ibid.* **63**, 061208 (2001).
[23]S. Danilov and D. Gurarie, ''Rhines scale and spectra of the β-plane turbulence with bottom drag,'' Phys. Rev. E **65**, 067301 (2002).
[24]S. Danilov and V. Gryanik, ''Vorticity structure and energy spectra in quasi-stationary beta-plane turbulence with a strong zonal component,'' Alfred Wegener Institute for Polar and Marine Research, Report No. 107 (2002).
[25]A different pattern (Karman-type vortex street) arises under stationary forcing, like the four-mode source of Ref. 16.
[26]V. Borue, ''Inverse energy cascade in stationary two-dimensional homogeneous turbulence,'' Phys. Rev. Lett. **72**, 1475 (1994).
[27]D. K. Lilly, ''Numerical simulation studies of two-dimensional turbulence: I. Models of statistically steady turbulence,'' Geophys. Fluid Dyn. **3**, 289 (1972).
[28]L. M. Smith and V. Yakhot, ''Finite-size effects in forced two-dimensional turbulence,'' J. Fluid Mech. **274**, 115 (1994).
[29]Some corrections are required in the vicinity of spectral peak k_p.
[30]T. G. Shepherd, ''Nonergodicity of inviscid two-dimensional flow on a beta-plane and on the surface of a rotating sphere,'' J. Fluid Mech. **184**, 289 (1987).
[31]A. J. Manfroi and W. R. Young, ''Slow evolution of zonal jets on the beta plane,'' J. Atmos. Sci. **56**, 784 (1999).
[32]G. R. Stuhne, ''One-dimensional dynamics of zonal jets on rapidly rotating spherical shells,'' Physica D **149**, 4379 (2001).
[33]A steep rise of ''constant'' C_z above $k=40$ is due to the ''background noise.''